Int. J. Heat Mass Transfer. Vol. 23, pp. 63–71
© Pergamon Press Ltd. 1980. Printed in Great Britain

0017-9310/80/0101-0063 $02.00/0

HEAT TRANSFER FROM A HIGH TEMPERATURE CONDENSABLE MIXTURE

S. H. CHAN†
Energetics Department, University of Wisconsin—Milwaukee, Milwaukee, WI 53201, U.S.A.

and

D. H. CHO and D. W. CONDIFF
Reactor Analysis and Safety Division, Argonne National Laboratory, Argonne, IL 60439, U.S.A.

(*Received* 23 *October* 1978 *and in revised form* 23 *February* 1979)

Abstract—Bulk condensation and heat transfer in a very hot gaseous mixture that contains a vapor component condensable at high temperature are investigated. A general formulation of the problem is presented in various forms. Analytical solutions for three specific cases involving both one- and two-component two-phase mixtures are obtained. It is shown that a detached fog formation is induced by rapid radiative cooling from the mixture. The formation of radiatively induced fog is found to be an interesting and important phenomenon as it not only exhibits unique features different from the conventional diffusion induced fog, but also greatly enhances heat transfer from the mixture to the boundary.

NOMENCLATURE

$B_{\lambda w}$, surface radiosity [W/cm²/cm];
$\hat{C}$, molar concentration $(C_1 + C_2)$ [mol/cm³];
C_i, ith component molar concentration [mol/cm³];
$\hat{C}_p$, molar specific heat at constant pressure [ergs/g K];
D, diffusion coefficient [cm²/s];
$e_{b\lambda}$, spectral black body emissive power [W/cm²/cm]
E_i, exponential integral of ith kind;
k, conductivity [W/cm K];
k_a, absorption coefficient [1/cm];
n, mass flux [g/cm² s];
N, molar flux [mol/cm² s];
P, pressure [Pa];
q_r, radiative flux [W/cm²];
r, mass fog production rate/volume [g/cm³ s];
R, molar fog production rate/volume [mol/cm³ s];
t, time [s];
u, mass average velocity [cm/s];
u^*, molar average velocity [cm/s];
W_λ, albedo of scattering;
x_i, ith component molar fraction;
z, physical coordinate normal to the wall [cm].

Greek symbols

α, vapor void fraction;
ε_λ, spectral emissivity;
λ, latent heat of condensation [ergs/g] or wavelength [cm];
Λ, molar latent heat of condensation [ergs/mol];
ρ, superficial mass density $(\rho_1 + \rho_2)$ [g/cm³];
ρ_i, ith component superficial mass density [g/cm³];
ρ^*, true mass density [g/cm³];
σ, Stefan Boltzmann constant [g/K⁴ s³];
τ, optical coordinate $(k_a z)$;
ω_i, ith component mass fraction.

Subscripts

0, initial condition;
1, condensable vapor;
2, noncondensable gas;
3, fog condensate;
∞, condition at infinity;
l, liquid;
w, wall;
v, vapor;
λ, wavelength [cm].

INTRODUCTION

THE PRESENT work reports a development in heat transfer that apparently has not been addressed before. It is concerned with heat transfer from a gaseous mixture that contains a condensable vapor and is at very high temperature. In the past, what has been investigated is the heat transfer associated with either a condensable mixture at low temperature or a noncondensable mixture at high temperature. The former reduces to the classical problem of fog formation in, say, atmosphere where the rate of condensation is diffusion controlled (molecular or conductive diffusions). In the presence of noncondensable gases, heat transfer to a cooler boundary by this mechanism is known to be drastically

†To whom correspondence should be directed.

reduced. In the latter case, where the high temperature mixture is noncondensable, radiative transfer may become dominant and a vast amount of existing literature belongs to this class of problem.

We consider here a fundamentally different type of problem of relevance to recent advances in open cycle MHD power plants and breeder reactor safety. In the advanced coal fired power plant using MHD as a topping cycle, a condensable mixture is encountered at temperatures of 2000–3000 K [1–4]. Condensation of the vaporized slag and seed materials at such a high temperature can take place in the MHD generator channel as well as in the radiant boiler. Similarly, in breeder reactor accident analyses involving hypothetical core disruptive accidents, a UO_2 vapor mixture at 4000 K or higher is often considered [5–9]. Since the saturation temperature of UO_2 at one atmosphere is close to 4000 K, condensation is also likely at a very high temperature. Accordingly, an objective of the present work is to provide an understanding of heat transfer and condensation mechanics in systems containing a high temperature condensable mixture.

Physically, as a high temperature condensable mixture is in contact with a cooler surface, a thermal boundary layer develops rapidly because of intensive radiative cooling from the mixture. Within this layer, the vapor becomes supersaturated and condenses to form fog before it can diffuse to the surface. To be seen in the present study, such a radiatively controlled fog formation, because of its action-at-a-distance characteristics, exhibits characteristics that are absent in the conventional diffusion induced fog formation processes. In addition to altering the radiative properties, the fog formation process itself offers a temperature sustaining mechanism.

By virtue of the high latent heat effects of condensation relative to sensible heat effects, a temperature will be maintained at high levels even under conditions of rapid radiative heat removal, which in turn is supportive of the heat transport mechanisms, resulting in a great enhancement of heat transfer to the surrounding wall.

GENERAL FORMULATION

In the following, a general formulation of the problem is given, which presents the species, energy and radiative transfer equations in readily usable forms. They will then be applied to three specific problems which will be solved analytically.

Consider a gas mixture made up of component 1, condensable vapor; component 2, noncondensable gas; and component 3, the condensate or fog. The conservation equations of species are [10]

$$\frac{\partial C_1}{\partial t} + \nabla \cdot N_1 = R_1 \tag{1}$$

$$\frac{\partial C_2}{\partial t} + \nabla \cdot N_2 = 0 \tag{2}$$

$$\frac{\partial C_3}{\partial t} + \nabla \cdot N_3 = R_3 \tag{3}$$

where $R_3 = -R_1 = R$ is the molar fog production rate per unit volume. Assuming that the fog occupies a negligible volume, that it moves at the molar-average velocity, and that it does not interfere with the diffusion of components 1 and 2, we can adopt a pseudo-binary approach whereby we define $\hat{C} = C_1 + C_2$, $x_i = C_i/\hat{C}$ for $i = 1, 2$ and 3. Introducing $N_1 = x_1 \hat{C} u^* - \hat{C} D \nabla x_1$, and making use of the identities, $\hat{C} u^* = N_1 + N_2$ and $\mathrm{D}^*/\mathrm{D}t = \partial/\partial t + u^* \cdot \nabla$, the combination of equations (1) and (2) eventually leads to

$$\hat{C} \frac{\mathrm{D}^* x_1}{\mathrm{D}t} = \nabla \cdot (\hat{C} D \nabla x_1) - (1 - x_1) R \tag{4}$$

Similarly, we have

$$\hat{C} \frac{\mathrm{D}^* x_2}{\mathrm{D}t} = \nabla \cdot (\hat{C} D \nabla x_2) \tag{5}$$

and

$$\hat{C} \frac{\mathrm{D}^* x_3}{\mathrm{D}t} = (1 + x_3) R \tag{6}$$

for components 2 and 3, respectively. In equation (6) the diffusion term disappears, for we assume the fog moving at the molar-average velocity.

In the presence of a net bulk motion, the species equations based on mass units rather than molar units are preferable in order to avoid the fictitious molar average velocity. They are:

$$\frac{\partial \rho_1}{\partial t} = -\nabla \cdot n_1 - r \tag{7}$$

$$\frac{\partial \rho_2}{\partial t} = -\nabla \cdot n_2 \tag{8}$$

$$\frac{\partial \rho_3}{\partial t} = -\nabla \cdot n_3 + r \tag{9}$$

or, in terms of mass fraction,

$$\rho \frac{\mathrm{D}\omega_1}{\mathrm{D}t} = \nabla \cdot D \rho \nabla \omega_1 - (1 - \omega_1) r \tag{10}$$

$$\rho \frac{\mathrm{D}\omega_2}{\mathrm{D}t} = \nabla \cdot D \rho \nabla \omega_2 \tag{11}$$

and

$$\rho \frac{\mathrm{D}\omega_3}{\mathrm{D}t} = (1 + \omega_3) r \tag{12}$$

respectively, where $\mathrm{D}/\mathrm{D}t \equiv \partial/\partial t + u \cdot \nabla$, $\rho u \equiv n_1 + n_2$, $\rho \equiv \rho_1 + \rho_2$ and $\omega_i \equiv \rho_i/\rho$ for $i = 1, 2$ and 3.

In one-component, two-phase systems where the mixture consists of a vapor and its own condensate, a common practice is to use void fraction in place of mass fraction. Designating the vapor void fraction by α, then the superficial vapor density ρ_v can be related to the true density ρ_v^* by $\rho_v = \alpha \rho_v^*$ and, similarly, $\rho_l = (1 - \alpha)\rho_l^*$ for the condensate. With $n_v = \rho_v u_v$ and $n_l = \rho_l u_l$ the two-phase continuity equations (7) and (9) can be re-cast into the following useful forms,

$$\frac{\partial}{\partial t}(\rho_v^* \alpha) = -\nabla \cdot (\alpha \rho_v^* u_v) - r \tag{13}$$

and

$$\frac{\partial \alpha}{\partial t} = \nabla \cdot [(1-\alpha)u_l] - \frac{r}{\rho_l^*} \tag{14}$$

where the true density of liquid condensate has been taken as constant.

The formulation is incomplete without specifying the energy equation, as the fog formation term in the species equation is governed mainly by the cooling rate. Assuming negligible viscous and diffusion dissipation effects, the energy equation can be written as

$$\hat{C}\hat{C}_p \frac{\mathrm{D}^* T}{\mathrm{D}t} = \nabla \cdot K \nabla T + \lambda r - \nabla \cdot q_r \tag{15}$$

where

$$\hat{C}_p = \sum_{i=1}^{3} x_i \hat{C}_{pi},$$

and q_r represents the radiative heat flux which augments conductive and convective heat transfer. Thus, the term $\nabla \cdot q_r$ represents a sink term attributed to radiative cooling.

In the present study, three specific problems will be investigated, all of which involve a semi-infinite mixture in contact with a cooler boundary. Under this configuration the divergence of radiative flux can be explicitly expressed by [11],

$$-\frac{\mathrm{d}q_r}{\mathrm{d}\tau} = 2\int_0^\infty B_{\lambda w} E_2(\tau_\lambda)\,\mathrm{d}\lambda + 2\int_0^\infty \int_0^\infty \times \left[(1-W_\lambda)e_{b\lambda}(\tau'_\lambda) + \frac{W_\lambda}{4} G_\lambda(\tau'_\lambda)\right] \times E_1(|\tau_\lambda - \tau'_\lambda|)\,\mathrm{d}\tau'_\lambda\,\mathrm{d}\lambda - \int_0^\infty [4(1-W_\lambda)e_{b\lambda}(\tau_\lambda) - W_\lambda G_\lambda(\tau_\lambda)]\,\mathrm{d}\lambda. \tag{16a}$$

Assuming a diffusive bounding surface, the spectral surface radiosity is given by

$$B_{\lambda w} = \varepsilon_{\lambda w} e_{b\lambda w} + 2(1-\varepsilon_{\lambda w}) \times \int_0^\infty \left[(1-W_\lambda)e_{b\lambda}(\tau'_\lambda) + \frac{W_\lambda}{4} G_\lambda(\tau'_\lambda)\right] \times E_2(\tau'_\lambda)\,\mathrm{d}\tau'_\lambda \tag{16b}$$

and the incident radiant energy per unit area within the mixture by

$$G_\lambda(\tau_\lambda) = 2B_{\lambda w} E_2(\tau_\lambda) + \tfrac{1}{2}\int_0^\infty G_\lambda(\tau'_\lambda) E_1(|\tau_\lambda - \tau'_\lambda|)\,\mathrm{d}\tau'_\lambda. \tag{16c}$$

In the above equations, W_λ is the spectral albedo of scattering, τ_λ is the optical thickness, E_n is the exponential integral function of order n and $e_{b\lambda}$ the spectral black body emissive power. It is noted that $B_{\lambda w}$, G_λ and $e_{b\lambda}$ all contain implicitly the unknown temperature profile by which the nonlinear integral equations (16a–c) are coupled to the transient differential equations (the species and energy equations). Thus analytical solutions appear to be difficult to obtain when the radiative transfer is included.

SOLUTIONS

In this section, some highly simplified problems are examined, which can nevertheless elucidate the essence of radiatively induced fog formation in a high temperature condensable mixture.

The semi-infinite condensable mixture is assumed to be in local thermodynamic equilibrium, bounded by a black surface. Thermophysical properties of individual constituents in the mixture are assumed to be constant. We further introduce the assumptions that the mixture is gray, radiation properties are constant and the albedo is negligibly small. The last assumption, though somewhat arbitrary, could be realized in a dilute mixture where the scattering coefficient is much smaller than the absorption coefficient. Even in cases where the albedo is not negligibly small, its effect on overall heat transfer is often less important than that of absorption. With these simplifications, equations (16a–c) are reduced to:

$$-\frac{\partial q_r}{\partial \tau} = 2\sigma T_w^4 E_2(\tau) + 2\int_0^\infty \sigma T^4(\tau') E_1(|\tau - \tau'|)\,\mathrm{d}\tau' - 4\sigma T^4(\tau). \tag{17}$$

This form will be used extensively in the problems to be solved next.

1. *Single-component two-phase mixture with no relative slip*

The first specific problem under consideration is a saturated semi-infinite mixture composed of a pure vapor and its own liquid droplets uniformly dispersed inside the mixture (see Fig. 1a). Being initially at a uniform saturation temperature T_∞ and pressure P_∞, the mixture is suddenly brought into contact

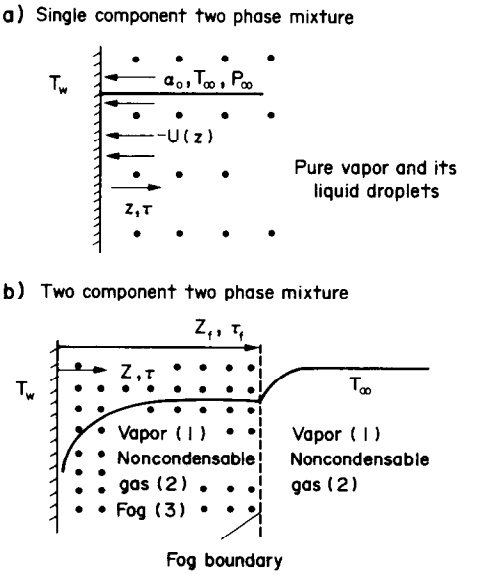

FIG. 1. Physical coordinates for single- and two-component two-phase mixture.

with a cooler surface at T_w. The case of no slip (i.e. $u_v = u_l = u$) between the vapor and droplets is considered here; complete slip will be treated in the following sub-section.

In view of the equilibrium condition and the semi-infinite extent, the temperature and pressure distributions within the mixture should remain approximately unchanged throughout the course of heat transfer, i.e. $DT/Dt = \nabla T = 0$. Then the species and energy equations (13)–(17) reduce to

$$\frac{\partial \alpha}{\partial t} = -\frac{\partial}{\partial z}(\alpha u) - \frac{r}{\rho_v^*} \tag{18}$$

$$\frac{\partial \alpha}{\partial t} = \frac{\partial}{\partial z}[(1-\alpha)u] - \frac{r}{\rho_l^*} \tag{19}$$

$$\lambda r - \frac{\partial q_r}{\partial z} = 0 \tag{20a}$$

and

$$\frac{\partial q_r}{\partial \tau} = 2\sigma(T_\infty^4 - T_w^4)E_2(\tau) \tag{20b}$$

where z and τ are measured from (normal to) the wall. Conduction heat transfer is assumed to be negligibly small in comparison with radiative transfer.

Apparently the heat transfer to the wall is $\sigma(T_\infty^4 - T_w^4)$ from equation (20b), and the local fog formation rate is

$$r = \frac{2\sigma k_a}{\lambda}(T_\infty^4 - T_w^4)E_2(\tau) \tag{21a}$$

from equation (20a). The total fog production rate is

$$r_{\text{total}} = \int_0^\infty r\,dz = \sigma(T_\infty^4 - T_w^4)/\lambda \tag{21b}$$

as is expected. The migration velocity of the vapor to replenish the vapor depleted due to condensation near the surface can also be readily obtained. Combination of equations (18) and (19) gives

$$\frac{\partial u}{\partial z} = -\left(\frac{1}{\rho_v^*} - \frac{1}{\rho_l^*}\right)r.$$

With the condition that $u = 0$ at $z = 0$ for all t, we can integrate to obtain

$$u = -u_\infty[1 - 2E_3(\tau)]. \tag{22}$$

Clearly $u_\infty \equiv \sigma(T_\infty^4 - T_w^4)(1/\rho_v^* - 1/\rho_l^*)/k_a\lambda$ represents the mixture velocity far away from the boundary. Since u_∞ is inversely proportional to the absorption coefficient k_a, a vapor with a higher opacity induces a smaller bulk motion because of self-shielding effects. Furthermore u_∞ is proportional to the fourth power of temperature, a unique characteristic that arises when radiative transfer is dominant.

With some stipulations, the vapor void fraction can be obtained analytically. Upon substitution of equation (21) into (18), there results

$$\frac{\partial \alpha}{\partial t} + u\frac{\partial \alpha}{\partial z} = \frac{\partial u}{\partial z}(\alpha_s - \alpha) \tag{23}$$

where $\alpha_s \equiv \rho_l^*/(\rho_l^* - \rho_v^*) \simeq 1$ for practical purposes. The general solution is equivalent to that of the two independent differential equations

$$\frac{dt}{1} = \frac{dz}{u} = \frac{d\alpha}{(\alpha_s - \alpha)\,du/dz} \tag{24}$$

with equation (22).

These characteristic equations must be integrated from the initial curve defined by $\alpha = \alpha_0$ at $t = 0$, i.e. along the z axis of the z–t plane. The solution is a set of curves represented by

$$t = -\int_z^{z_0} \frac{dz}{u} \tag{25}$$

$$(\alpha_s - \alpha)u = (\alpha_s - \alpha_0)u_0 \tag{26}$$

where z_0 is the initial value of z (at $t = 0$) along the characteristic, so that z_0 identifies the characteristic, and u_0 is u at $z = z_0$, as obtained from (22). Since $u = 0$ at $z = 0$ it follows that, from equation (26), $\alpha = \alpha_s$ at the cold wall for all time $t > 0$. An α vs z profile at fixed time is obtained by eliminating z_0 between (25) and (26) utilizing (22).

An explicit expression for α is obtainable if the standard exponential kernel approximation is employed whereby $E_3(\tau)$ is replaced by an exponential function of the form $(1/2)\exp(-3\tau/2)$. By substituting equation (22) into equation (25) and evaluating the integral in accordance with the exponential kernel approximation, we obtain

$$e^{3\tau_0/2} - 1 = (e^{3\tau/2} - 1)e^{3k_a u_\infty t}.$$

Using equation (26), along with the above equation and the simplified form $u = u_\infty(e^{-3\tau/2} - 1)$ and $u_0 = u_\infty(e^{-3\tau_0/2} - 1)$ of (22), to eliminate τ_0 and u_0, we obtain the final solution

$$\frac{\alpha_0 - \alpha_s}{\alpha - \alpha_s} = 1 - e^{-3\tau/2}(1 - e^{-3u_\infty k_a t/2}). \tag{27}$$

It is interesting to observe that the results are given in terms of exponential functions. This exponential behavior is distinctively different from the square root nature in existing fog formation solutions based on diffusion mechanisms. The migration velocity profile given by equation (22) is responsible for this and can be understood on simple physical grounds. Inasmuch as the replenished mass flux at a given optical coordinate τ is linearly proportional to the net radiative heat loss from the layer between $\tau = 0$ and $\tau = \tau$, the migration velocity at τ should be linearly proportional to the emissivity (or absorptivity) of the gas layer. Since the emissivity of an optically thick layer is unity and $[1 - 2E_3(\tau)]$ for a finite layer, the ratio of migration velocities, $u(\tau)/u_\infty$, should be identical to the emissivity of the layer as given by equation (22). The fog formation rate and the migration velocity, both being time independent, are presented in Fig. 2, with the liquid void fraction in Fig. 3. For comparison purposes, the complete slip solutions are superimposed in the figures. A discussion on their differences and similarity is presented in the following section.

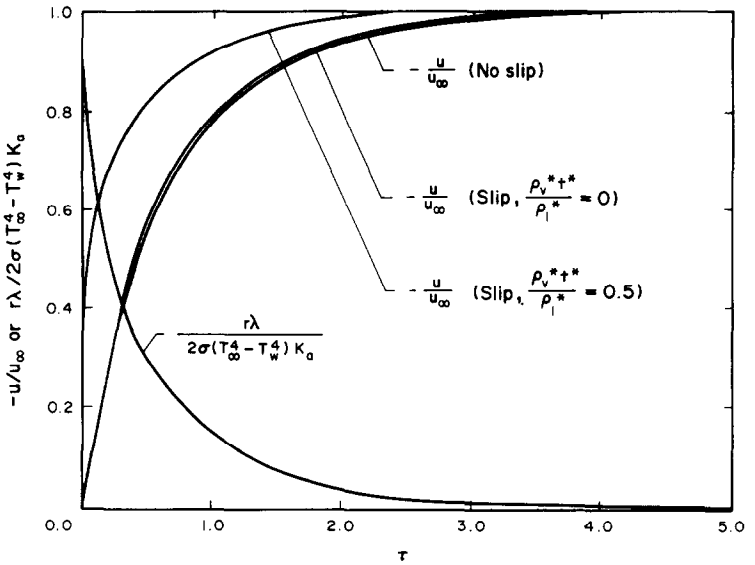

FIG. 2. Local fog formation rate and local mass average velocity distribution in a single-component two-phase mixture.

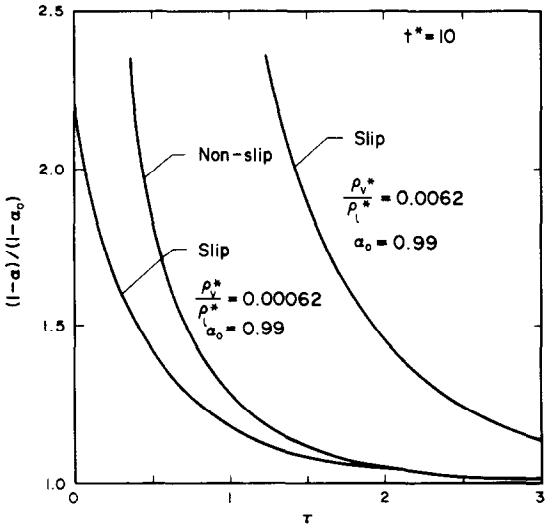

FIG. 3. Liquid void fraction distribution in a single-component two-phase mixture.

2. *Single-component two-phase mixture with slip*

We now extend to the opposite case of allowing a complete slip between the vapor and condensate, i.e. $u_l = 0$ and $u_v = u$. In this case the continuity equations are simplified to

$$\frac{\partial \alpha}{\partial t} = -\frac{\partial}{\partial z}(\alpha u) - \frac{r}{\rho_v^*} \tag{28}$$

$$-\frac{\partial \alpha}{\partial t} = \frac{r}{\rho_l^*}. \tag{29}$$

The energy equation remains unchanged, so are the resulting heat transfer and fog formation rates. The vapor void fraction and velocity equations can be easily solved to yield

$$\alpha = \alpha_0 - \frac{r}{\rho_l^*} t \tag{30a}$$

or

$$(1-\alpha)/(1-\alpha_0) = 1 + 2E_2(\tau)(\rho_v^*/\rho_l^*)t^*/(1-\alpha_0) \tag{30b}$$

where $t^* \equiv u_\infty K_a t$ and

$$u = -u_\infty[1 - 2E_3(\tau)]/\alpha \tag{31}$$

respectively.

In comparison with the no-slip case, we see that whether there is slip or not has no effect on fog production or heat-transfer rate. However the vapor migration velocity profiles in the mixture given by equations (22) and (31) are different by a factor of α. Since $\alpha \leqslant 1$ and is time dependent, the migration velocity in the slip case becomes transient and is larger. Furthermore, the liquid void fraction $(1-\alpha)$, is linearly proportional to time in the slip case, but not in the non-slip case. In the former, the liquid being frozen in place can only be increased by condensation. Since the condensation rate is constant with respect to time, it leads to a linear time dependent void fraction. From Fig. 2, we see that the slip solution gives rise to a larger migration velocity. However, depending on the initial void fraction and the vapor–liquid density ratio, it can go either way in the liquid void fraction as illustrated in Fig. 3.

3. *Two-component two-phase mixture*

We now turn to a more difficult example problem involving a two-component mixture, with one-component noncondensable. The noncondensable gas complicates the matter considerably as it impedes the motion of condensable vapor toward the fog region and thus, creates a nonuniform and non-steady temperature distribution within the mixture as shown in Fig. 1b.

For generality, we allow the mixture to be uniformly superheated initially. After the mixture adjacent to the surface cools to its saturation

temperature, condensation will occur and two distinct regions, fog and fog-free regions, will appear. We then have to solve conservation equations in each region and match solutions together.

To keep the problem amenable, we assume that bulk convection, conduction and molecular diffusion are negligibly small in comparison with the effects attributable to thermal radiation. This assumption appears to be reasonable in view of the high temperature of the mixture which intensifies the radiation. In addition, it is assumed that the mixture is in local thermodynamic equilibrium and that the gas and vapor obey the ideal gas law.

In the absence of bulk velocity, the molar formulation, equations (4)–(6), (15), is preferable. In the fog free region, $R = x_3 = 0$, $\hat{C} = \hat{C}_0 = \text{constant}$ and

$$\frac{\partial x_1}{\partial t} = 0 \tag{32}$$

$$\hat{C}\hat{C}_p \frac{\partial T}{\partial t} = \frac{\partial q_r}{\partial z} \tag{33}$$

for $z_f \leqslant z$ where z_f indicates the fog layer thickness which grows with time. The divergence of radiative flux given by equation (17) is still applicable. Similarly in the fog region we have

$$\hat{C}\frac{\partial x_1}{\partial t} = -(1-x_1)R \tag{34}$$

$$\hat{C}\frac{\partial x_3}{\partial t} = (1+x_3)R \tag{35}$$

$$\hat{C}\hat{C}_p \frac{\partial T}{\partial t} = \Lambda R + \frac{\partial q_r}{\partial z} \tag{36}$$

for $0 \leqslant z \leqslant z_f$.

Exact analytical solutions do not seem possible as they involve a system of transient differential integral equations. Consequently, we must resort to numerical or approximate analytical techniques wherever plausible. We attempt to solve x_1 and x_3 in terms of T first, and then obtain solutions for T.

Vapor molar fraction

The vapor molar fraction in the fog free region is obvious from equation (32); it is constant and uniform, at its initial value x_{10}.

In the fog region, by eliminating R between equations (34) and (35), we have

$$-\frac{1}{1-x_1}\frac{\partial x_1}{\partial t} = \frac{1}{1+x_3}\frac{\partial x_3}{\partial t}$$

which is subject to the condition that at $t = t_f$, $x_1 = x_{\text{sat}}$ and $x_3 = 0$. The physical meaning of the condition can be best understood by referring to Fig. 4, which shows how the thickness of fog grows with time. At the time $t = t_f$ the fog boundary is located at $z = z_f$ (or $\tau = \tau_f$). At the boundary, the fog vanishes, i.e. $x_3 = 0$, and the vapor is saturated, namely $x_1 = x_{\text{sat}}(T_{\text{sat}}) = \text{constant}$, where T_{sat} is the saturation temperature corresponding to the vapor pressure P_∞ in the fog-free region which stays constant.

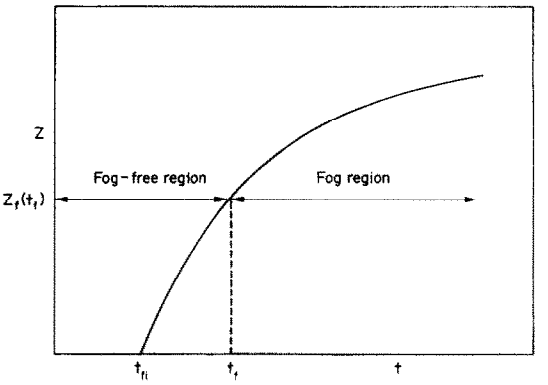

FIG. 4. Fog formation region and the thickness of fog layer.

Integration of the above equation yields

$$\frac{1-x_1}{1-x_{\text{sat}}} = 1+x_3. \tag{37}$$

Because $\hat{C}(1+x_3) = C_1+C_2+C_3 = \hat{C}_0 = \text{constant}$ and $\hat{C} = P_v(T)/x_1 RT$, the final result is

$$x_1(T) = g_0(T)/[1-x_{\text{sat}}+g_0(T)] \tag{38}$$

and, consequently, from equation (37)

$$x_3(T) = [x_{\text{sat}}-g_0(T)]/[1-x_{\text{sat}}+g_0(T)] \tag{39}$$

where

$$g_0(T) \equiv C_1/\hat{C}_0 = P_v(T)/\hat{C}_0 RT.$$

If the Clasius–Clapeyron type of equation is supplied for $P_v(T)$ and the temperature profile known, the local molar fractions can be evaluated from equations (38) and (39). Other related quantities such as local fog concentration $C_3 = \hat{C}x_3 = \hat{C}_0[x_{\text{sat}}+g_0(T)]$ and total fog produced,

$$\int_0^{Z_f} C_3\,\mathrm{d}Z,$$

can be calculated in a straightforward manner when needed.

Temperature profile and fog layer thickness

Turning now to the transient temperature distribution, a major mathematical difficulty arises from the integral form of the radiative flux expression. However, great simplification can be realized in cognizance of the fact that $E_1(|\tau'-\tau|)$ behaves as a delta function. As $\tau' \to \tau$, $E_1 \to \infty$ and as $|\tau'-\tau|$ increases, E_1 diminishes rapidly. As a result equation (17) can be approximated by

$$\begin{aligned}-\frac{\mathrm{d}q_r}{\mathrm{d}\tau} &\simeq 2\sigma T_w^4 E_2(\tau)+2\sigma T^4(\tau)\int_0^\infty E_1(|\tau-\tau'|)\,\mathrm{d}\tau' \\ &\quad -4\sigma T^4(\tau) \\ &= 2E_2(\tau)\sigma[T_w^4-T^4(\tau)].\end{aligned} \tag{40a}$$

This approximation has been used and found to be satisfactory in our previous analyses [5, 8]. In the

present problem of interest, $T^4 \gg T_w^4$, thus

$$\frac{dq_r}{d\tau} \simeq 2\sigma T^4(\tau)E_2(\tau). \tag{40b}$$

Employing the above approximation in equation (33), the transient temperature profile in the fog-free region can be found, with the initial condition $T = T_\infty$ at $t = 0$, as

$$\theta^3 = 1/[1+3\beta E_2(\tau)t] \tag{41}$$

where $\theta = T/T_\infty$ and $\beta = 2k_a\sigma T_\infty^3/\hat{C}\hat{C}_p$. It should be noted that in the fog-free region

$$\hat{C}\hat{C}_p = \sum_{i=1}^{3} C_i\hat{C}_{pi} = \text{constant}$$

as C_i's are invariant and $\hat{C}_{pi}$'s were assumed as constant. However, in the fog region the C_i's changes with time.

Fog formation starts as soon as the temperature drops to the saturation temperature, T_{sat} corresponding to P_∞. Then setting $T = T_{sat}(P_\infty)$ or $\theta = \theta_{sat}$ in equation (41) yields the equation for the growth of fog layer thickness with time,

$$t_f = (\theta_{sat}^{-3} - 1)/3\beta E_2(\tau_f), \tag{42}$$

as depicted in Fig. 4.

In the fog region, some stipulations are necessary to obtain the temperature profile. By eliminating R between equation (34) and (36), and noting that under the local thermodynamic equilibrium,

$$\frac{\partial x_1}{\partial t} = x_1' \frac{\partial T}{\partial t} \tag{43}$$

where $x_1'(T) \equiv dx_1(T)/dT$, we have

$$\hat{C}\hat{C}_p \frac{\partial T}{\partial t} = \frac{\partial q_r/\partial Z}{1 + \dfrac{\Lambda x_1'}{\hat{C}_p(1-x_1)}} \tag{44}$$

for $t \geqslant t_f$ and $Z \geqslant Z_f$. Employing the same approximation from equation (40b), the above equation can be integrated from $t = t_f$ to t. If use is made of equation (42), the final temperature profile is found analytically and is implicitly given by

$$\beta E_2(\tau)t = \tfrac{1}{3}(\theta_f^{-3} - 1) + \int_\theta^{\theta_f} \frac{\eta(\theta)(1+\gamma(\theta))}{\theta^4}\,d\theta \tag{45}$$

in which $\theta \equiv T/T_\infty$, $\beta \equiv 2\sigma T_\infty^3 k_a/\hat{C}_\infty\hat{C}_{p\infty}$, $\gamma \equiv \Lambda x_1'(T)/\hat{C}_p(1-x_1(T))$ and $\eta(T) \equiv \hat{C}\hat{C}_p/\hat{C}_\infty\hat{C}_{p\infty}$. Since $\hat{C}_p$, $\hat{C}$ and x_1' are generally temperature dependent, they are provided below to facilitate later numerical computations,

$$\hat{C}_p = x_1\hat{C}_{p1} + x_2\hat{C}_{p2} + x_3\hat{C}_{p3}$$
$$= \hat{C}_{p2} + \frac{g_0(T)(\hat{C}_{p1} - \hat{C}_{p2}) + (X_{sat} - g_0(T))\hat{C}_{p3}}{1 - x_{sat} + g_0(T)}$$
$$\hat{C} = \hat{C}_0[1 - x_{sat} + g_0(T)]$$

and

$$x_1' = dx_1/dT = (1 - x_{sat})g_0'(T)/[1 - x_{sat} + g_0(T)]^2$$

where $g_0'(T) = dg_0/dT$. With these explicit analytical expressions, the integration term in equation (45) can be numerically carried out in a straightforward manner to yield the temperature distribution as a function of time and position in the fog region.

Wall heat flux

In the absence of conduction and convection, the radiative flux represents the total wall heat flux,

$$-q_{rw}(t) = 2\sigma T_\infty^4 \int_0^\infty \theta^4(\tau, t)E_2(\tau)\,d\tau. \tag{46a}$$

Prior to fog formation, i.e. $t < t_{fi}$ (see Fig. 4), θ is given by equation (41). Thus

$$-\frac{q_{rw}(t)}{2\sigma T_\infty^4} = \int_0^\infty \frac{E_2(\tau)}{[1+3\beta t E_2(\tau)]^{4/3}}\,d\tau \tag{46b}$$

which again calls for numerical integration. After fog formation, namely $t > t_{fi}$, two distinct regions appear. Accordingly,

$$-\frac{q_{rw}(t)}{2\sigma T_\infty^4} = \int_0^{\tau_f(t)} E_2(\tau)\theta^4(t,\tau)\,d\tau + \int_{\tau_f(t)}^\infty \frac{E_2(\tau)\,d\tau}{[1+3\beta t E_2(\tau)]^{4/3}}. \tag{46c}$$

The first term is attributable to the fog region with θ given by equation (45), while the second term is attributable to the fog-free region.

Illustration

As an application of the above solutions, we consider a large two-component two-phase bubble such as encountered in nuclear reactor safety. The bubble, which might arise in a hypothetical core disruptive accident of a breeder reactor, consists of UO_2 fuel vapor and a noncondensable gas of xenon with the following initial condition: UO_2 vapor pressure = 0.2655 MPa (which implies $T_{sat} = 4000$ K), total pressure = 0.3 MPa and 50 K superheat (i.e. $T_\infty = 4050$ K). The specific heats at constant pressure of UO_2 vapor, xenon gas and liquid condensate are taken as 20.02, 12.55 and 135.56 J/gmole K, respectively. The latent heat of condensation of UO_2 vapor is 5.19×10^5 J/gmole K and the saturation relationship between UO_2 vapor pressure and temperature is taken as

$$P_{sat} = 0.1\exp\left(69.979 - \frac{76\,800}{T_{sat}} - 4.34\ln T_{sat}\right)$$

where P_{sat} and T_{sat} are in units of Pa and K. In the absence of experimental data for UO_2 vapor, an absorption coefficient of 0.00082 cm^{-1} is assumed.

Figure 5 shows the transient temperature profile and fog penetration depth, τ_f, in the vicinity of a cold boundary. The sensible heat in the initially fog-free mixture rapidly radiates away to the cold wall, inducing an exponential growth of thermal boundary layer, which in turn triggers a fog formation. Solid lines in the sections below 4000 K correspond to the fog zones where the heat of condensation is released and delivered to the boundary by radiation. Other lines above 4000 K lie in the fog-free region, from

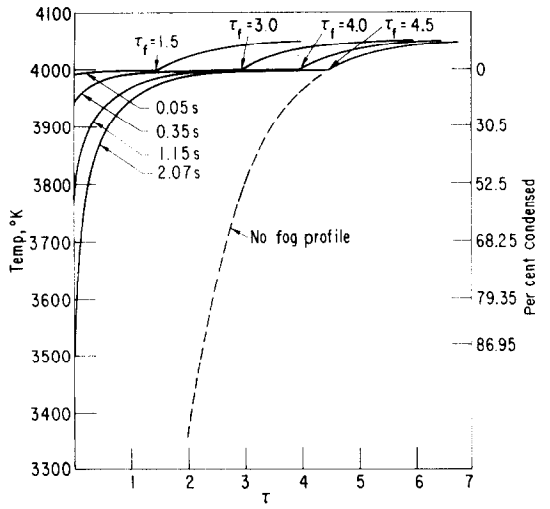

FIG. 5. Transient temperature profile and fog penetration depth.

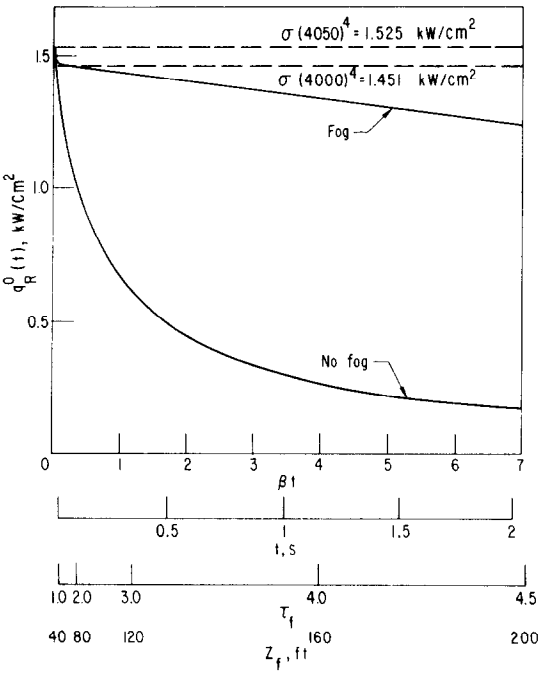

FIG. 6. Radiative flux to the cooler surface with and without fog formation.

which sensible heat is being radiated away. The very steep dashed line corresponds to the temperature profile at time 2.07 s if fog formation were not considered. Without the fog formation the temperature profile in the fog region departs substantially from the one with fog formation. Figure 6 shows the transient heat flux at wall vs time. The lower solid curve shows values predicted on neglect of fog formation while the upper solid curve shows the values with fog formation. For comparison purposes, black body emissions based on initial superheated temperature and saturated temperature are represented by dashed lines in the figure. We see the great significance of fog formation as it increases the flux by an order of magnitude by sustaining the flux. Thus the fog formation is an important factor that should be considered in calculating the heat transfer from a high temperature condensable mixture: the neglect of it could lead to a large error by grossly underestimating the flux.

SUMMARY

Analytical solutions for three specific problems relating to heat transfer from a high temperature condensable mixture have been obtained. Our results show that the rapid radiative cooling from the mixture induces a detached fog formation. This radiative controlled fog formation is a new and interesting phenomenon. We find it to be very effective in transferring heat to the cooler boundary because as the vapor condenses into fog in the mixture, the latent heat of condensation tends to sustain the temperature of fog which in turn enhances the heat transfer to the boundary by means of thermal radiation.

CONCLUDING REMARKS

While three solutions have been obtained to provide insight into heat transfer mechanism and radiatively controlled fog formation in high temperature condensable mixture, some idealizations were necessarily made in this paper to arrive at those solutions. They should be gradually relaxed in later studies. In particular, it would be of practical and fundamental interest to remove the assumption that the absorption coefficient is constant, by incorporating into analyses the dependence of both absorption and scattering coefficients on evolution of fog condensate.

Acknowledgement - This work was performed under the auspices of the U.S. Department of Energy.

REFERENCES

1. A. W. Postlethwaite and M. M. Sluyter, Heat transfer problems associated with an MHD power generation system—an overview, Presented at the A.I.Ch.E.-ASME Heat Transfer Conference, 77-HT-62, Salt Lake City, Utah, 15–17 August (1977).
2. W. D. Jackson, MHD electrical power generation: prospects and issues, AIAA 9th Fluid and Plasma Dynamics Conference, San Diego, California, 14–16 July (1976).
3. K. H. Im, P. M. Chung and L. W. Carlson, Slag and seed deposition on heat exchanger surfaces from gas–droplet mixtures, 17th Symposium on Engineering Aspects of MHD, Stanford, CA, March (1978).
4. K. H. Im and P. W. Chung, Nucleation and evolution of slag droplets in coal combustion, 17th Symposium on Engineering Aspects of MHD, Stanford, CA, March (1978).
5. S. H. Chan and D. H. Cho, A calculational method for transient radiation heat transfer in an absorbing–emitting medium and its application to LMFBR accident analysis, *Trans. Am. Nucl. Soc.* **21**, 323 (1975).
6. S. H. Chan and D. H. Cho, A preliminary assessment of the attenuation of HCDA radiological consequences by thermal radiation, *Trans. Am. Nucl. Soc.* **24**, 253 (1976).

7. S. H. Chan and D. H. Cho, Effect of radiative cooling on HCDA radiological consequences during buoyancy period, *Trans. Am. Nucl. Soc.* **26**, 340 (1977).
8. S. H. Chan and D. H. Cho, Transient radiative heat transfer between two emitting–absorbing media, in *Symposium of Sixth International Heat Transfer Conference, Toronto, Canada*, 7–11 August (1978).
9. D. W. Condiff and S. H. Chan, Studies of radiation controlled fog formation, *Trans. Am. Nucl. Soc.* **22**, 452 (1975).
10. R. B. Bird, W. E. Stewart and E. N. Lightfoot, *Transport Phenomena*. John Wiley, New York (1960).
11. E. M. Sparrow and R. D. Cess, *Radiation Heat Transfer*. Hemisphere, Washington (1978).

TRANSFERT THERMIQUE LORS DE LA CONDENSATION D'UN MELANGE CONDENSABLE ET A TEMPERATURE ELEVEE

Résumé—On étudie la condensation en masse et le transfert thermique pour un mélange de gaz très chaud qui contient une vapeur condensable à température élevée. On présente sous des formes différentes une formulation générale du problème. On obtient des solutions analytiques pour trois cas spécifiques correspondant à des mélanges à un ou deux composants et deux phases. On montre que la formation d'un brouillard est induite par un rapide refroidissement du mélange par rayonnement. La formation du brouillard induite par le rayonnement est un phénomène intéressant et important qui est un mécanisme différent de la formation conventionnelle par diffusion et qui augmente beaucoup le transfert thermique entre le mélange et les parois.

WÄRMEÜBERGANG VON EINEM BEI HOHER TEMPERATUR KONDENSIERBAREN GEMISCH

Zusammenfassung—Untersucht werden die Kondensation und der Wärmeübergang in einem sehr heißen Gasgemisch, wobei das Gemisch eine Dampfkomponente enthält, die bei hohen Temperaturen kondensierbar ist.

Eine allgemeine Formulierung des Problems wird in unterschiedlichen Darstellungen angegeben. Für drei spezifische Fälle, die sowohl Ein- als auch Zweikomponenten–Zweiphasengemische einschließen, erhält man analytische Lösungen.

Es wird gezeigt, daß durch schnelle Wärmeabfuhr durch Strahlung eine besondere Nebelbildung herbeigeführt werden kann. Die durch Strahlungsaustuasch bedingte Nebelbildung hat sich als eine interessante und wichtige Erscheinung erwiesen, und zwar nicht nur dadurch, daß sie besondere Eigenheiten aufweist, die sich von denen bei der üblichen, durch Diffusion hervogerufenen Nebelbildung unterscheiden, sondern auch dadurch, daß sie den Wärmeübergang von dem Gemisch an die Phasengrenze in hohem Maß begünstigt.

ТЕПЛОПЕРЕНОС ОТ СИЛЬНО НАГРЕТОЙ КОНДЕНСИРУЕМОЙ СМЕСИ

Аннотация — Исследуются объёмная конденсация и перенос тепла в сильно нагретой смеси газов, содержащей пар, конденсируемый при высокой температуре. Даны различные формулировки общей задачи. Получены аналитические решения для трёх частных случаев одно- и двухкомпонентных двухфазных смесей. Показано, что образование тумана происходит в результате быстрого охлаждения смеси вследствие излучения. Данное явление является весьма интересным и важным, поскольку оно не только отличается от процесса образования тумана за счёт обычного диффузионного процесса, но также оказывает большое влияние на интенсификацию переноса тепла от смеси к границе.